Dispersion and Field Analysis of a Microstrip Meander-Line Slow-Wave Structure

JERALD A. WEISS, SENIOR MEMBER, IEEE

Abstract—**A structure which is important as an example of a spatially periodic medium for microwave propagation is analyzed theoretically, with rigorous consideration of its partial dielectric composition, symmetry properties, and field configuration relating to its use for electron-wave interaction in a crossed-field amplifier (CFA). The analysis is carried out in a quasi-TEM approximation, leading to determination of a complex potential function within the unit cell and the associated normal-mode parameters: effective dielectric constant, phase velocity, and characteristic impedance, as functions of phase per cell and mode symmetry. With imposition of meander-line boundary conditions, solutions of the characteristic equation for the dispersion law of the structure are computed, including the influence of the inhomogeneous dielectric-vacuum construction of microstrip. Agreement with the observed phase and stopband features of a representative structure is very good. Power distribution and group velocity are calculated, and an interaction impedance, representing the coupling between the RF field and an electron beam for estimation of CFA performance is also calculated. The method lends itself to detailed computations, including the effects of structural features of practical slow-wave circuits.**

I. INTRODUCTION

THE PASSAGE of electromagnetic radiation through spatially periodic media arises in a variety of physical situations, including some as widely diverse as X-ray diffraction by crystals, transmission and reception by microwave array antennas, optical integrated circuits, and RF filtering. From consideration of the symmetry properties of the medium and the logical consequences of these, it is possible to deduce certain qualitatively distinctive features, such as the existence of stopbands, properties of the dispersion function, and angular diffraction lobe patterns. For most applications, however, the generation of useful design information and the realistic comparison of theoretical and experimental results are possible only if the boundary-value problems involved can be solved in a substantially rigorous manner. With the aid of symmetry principles the problem can be reduced to that of field analysis in a single unit cell of the periodic medium. This reduced problem may itself be a rather formidable task, and the value of the results depends on the recognition and analysis of the effects of significant structural parameters. Various simplified versions of the slow-wave structure for the vacuum-tube crossed-field amplifier (CFA) have been treated in the microwave literature [1], [2]. The objective of the present analysis is to calculate the dispersion function, iterative and interaction impedances, and other details of the microstrip meander line, incorporating the dielectric and conductor configuration in sufficient detail to permit a realistic assessment of the electrical effects of design variations which might be introduced in order to fulfill the practical CFA design constraints.

Manuscript received May 2, 1974; revised August 27, 1974. This work was supported by the Department of the Army.

The author is with the Department of Physics, Worcester Polytechnic Institute, Worcester, Mass. 01609, and Lincoln Laboratory, Massachusetts Institute of Technology, Lexington, Mass. 02173.

II. THE QUASI-TEM MODEL

The propagation medium contemplated for the analysis of the microstrip meander line is an infinite array of parallel strips on a shielded grounded dielectric substrate, as illustrated in Fig. 1. As indicated in the figure, the meander line will be considered to occupy a region of width A, with conducting links connecting the ends of adjacent strips alternately at the two sides of that region. With the electromagnetic fields satisfying boundary conditions appropriate to the configuration of conductor and dielectric, the remainder of the infinite array outside the region of interest may be discarded (or alternatively, as with guided-wave structures generally, it may be regarded as an infinite repetition of the same configuration of matter and of corresponding fields). The procedure will be to seek solutions of the wave equation on the complete infinite array which not only conform to the arrangement of its boundaries but also reflect its symmetry properties. The principal value of this approach, as contrasted for example with calculations which begin with the determination of the fields on an individual isolated strip, is that by this means the overlap and consequent coupling of fields are rigorously incorporated for neighboring strips of all orders.

The general form of the normal modes of propagation in the infinite array is that of waves having constant amplitude and uniform phase variation k per unit length in the x direction, parallel to the strips. In addition, as in the case of filters and other periodic networks generally, these modes are characterized by the parameter φ, denoting a constant phase increment per unit cell (dimension p) in the z direction, which becomes the resultant direction of propagation in the meander line. Thus the planes of constant phase make, in general, a slant angle $\pm\arctan(kp/\varphi)$ with the z axis, and for each value of φ there is a degenerate set of four such waves, corresponding to propagation directions in each of the four quadrants relative to the x and z axes. An additional two-fold degeneracy with respect to the parameter φ arises due to our choice of unit cell embracing two conducting strips; it is a manifestation of the reflection symmetry of the unit cell.

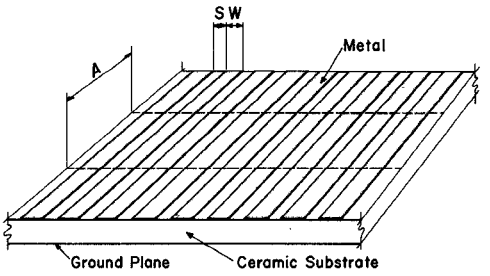

Fig. 1. An infinite array of parallel strips, with respect to which the symmetry-adapted normal modes of propagation are defined.

It should be noted that the foregoing symmetry properties are shared by all modes of propagation on the infinite microstrip array. The present analysis is limited, however, to the fundamental modes (to be defined later) which govern the behavior of the slow-wave structure in the frequency range which is of interest for most applications.

Determination of the normal modes of propagation is performed by a Green's function method in which the charge and current distribution on the conducting strips is rigorously determined also, thus yielding a capacitance per strip, an effective dielectric constant, and a characteristic impedance for each mode.

It then remains to obtain a superposition of the normal modes so as to fulfill the meander-line boundary conditions, at the connecting links between strips. Solution of this problem leads to determination of the relation between frequency and the phase parameter φ, i.e., the dispersion relation for the microstrip meander line. The wave field resulting from the superposition of modes may be intuitively visualized as a wave which propagates in meandering fashion, following the meandering conductor configuration. All the other quantities of interest are thereby determined, including the RF field configuration and all information required for study of the interaction with an electron beam.

To begin the analysis, we assume that propagation in the medium illustrated in Fig. 1 can be characterized by an effective dielectric constant K_{eff}, which depends on the mode of propagation considered. We assume that a wave function $\Phi(x,y,z)$ representing a mode in this medium satisfies a Helmholtz equation

$$\nabla^2\Phi + (\omega^2/c^2)K_{\text{eff}}\Phi = 0. \tag{1}$$

We further assume that it is a good approximation [3] to treat the modes as TEM with respect to the direction of the strips (x direction). Since the medium is uniform in the direction of the strips, it must be possible to find wave functions of the form

$$\Phi(x,y,z) = U(y,z) \exp(\pm ikx)$$

i.e., wave functions having the form of normal-mode functions, for which the effect of translation in the x direction is change of phase only. From (1), $U(y,z)$ satisfies

$$\frac{\partial^2 U}{\partial y^2} + \frac{\partial^2 U}{\partial z^2} + \left(\frac{\omega^2}{c^2}K_{\text{eff}} - k^2\right)U = 0. \tag{2}$$

According to the electromagnetic field equations, the assumption that the wave is TEM with respect to x implies

$$k^2 = (\omega^2/c^2)K_{\text{eff}}. \tag{3}$$

Hence U satisfies

$$\frac{\partial^2 U}{\partial y^2} + \frac{\partial^2 U}{\partial z^2} = 0. \tag{4}$$

We may take U to represent an electric potential defined in a two-dimensional manifold, namely, the yz plane.

Coordinate Axes: Having previously chosen x parallel to the (infinite) length of the strips, we take y upward, perpendicular to the substrate surface, and z horizontal and transverse to the strips. The grounded lower surface of the substrate is taken to be the xz plane. See Fig. 2.

Now, since the array of strips is periodic with respect to translation in the z direction, with period (unit cell dimension) p, there must exist solutions (Bloch functions [4]) in the form

$$U(y,z) = f(y,z) \exp(i\varphi z/p) \tag{5}$$

in which $f(y,z)$ is periodic with period p. In anticipation of the glide-plane symmetry of the meander-line configuration contemplated (Fig. 2) it is convenient to take the unit cell dimension p to embrace two neighboring strips. With (5), we have from (4),

$$\frac{\partial^2 f}{\partial y^2} + \frac{\partial^2 f}{\partial z^2} + 2i\frac{\varphi}{p}\frac{\partial f}{\partial z} - \frac{\varphi^2}{p^2}f = 0. \tag{6}$$

Fourier series expansion of the complex periodic function $f(y,z)$

$$f(y,z) = \sum_{m=-\infty}^{+\infty} F_m(y) \exp(2\pi imz/p). \tag{7}$$

Equation (6) yields the following equation for the Fourier coefficients $F_m(y)$:

$$\frac{d^2F_m}{dy^2} - \left(\frac{\varphi + 2\pi m}{p}\right)^2 F_m = 0. \tag{8}$$

Define β_m by

$$\beta_m = \frac{\varphi + 2\pi m}{p}.$$

Thus, according to (8), $F_m(y)$ is proportional to $\exp(\pm\beta_m y)$.

Using (5), (7), and (8), we may take U to be

$$U(y,z) = \begin{cases} \sum_m C_m \exp(i\beta_m z) \sinh|\beta_m| y, \\ \qquad\qquad 0 \le y \le H_1 \\ \sum_m D_m \exp(i\beta_m z) \sinh|\beta_m| (H_2 - y), \\ \qquad\qquad H_1 \le y \le H_2 \end{cases} \tag{9}$$

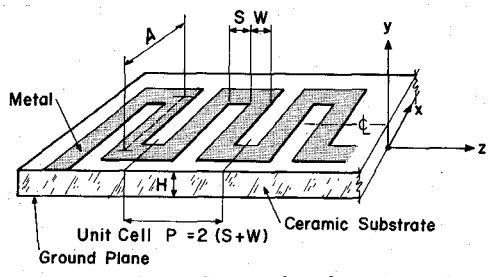

Fig. 2. Dimensions and coordinates for the microstrip meander line, showing the unit cell.

where H_1 and H_2 are, respectively, the heights of the substrate surface and upper shield plane above the bottom ground plane. Determination of the coefficients C_m and D_m follows from the boundary conditions on U and on $D_y = K\epsilon_o(-\partial U/\partial y)$ at the substrate surface. Continuity of U yields

$$\frac{D_m}{C_m} = \frac{\sinh \mid \beta_m \mid H_1}{\sinh \mid \beta_m \mid (H_2 - H_1)}. \tag{10}$$

III. THE GREEN'S FUNCTION

Considering the unit cell and its boundaries, we proceed to solve the boundary-value problem for the scalar potential $U(y,z)$. If the configuration of the conductor and dielectric boundary are complicated (as in the case of some CFA slow-wave structures where the dielectric substrate is slotted or is made in the form of a series of disjoint bars, or where the thickness of the conducting strips cannot be neglected), then it is necessary to resort to methods involving finite difference, image, discrete Green's function, or other numerical techniques [5] for determination of $U(y,z)$. In the present discussion we shall illustrate the principles of the formulation by considering a simple microstrip structure in which the substrate–vacuum interface is flat and in which the strip thickness is negligible. In this case the imposition of boundary conditions for determination of the periodic function $f(y,z)$, expressed as a Fourier series in (7), can be carried out directly.

The unit cell contains two strips. Hence, for each value of φ there exist two linearly independent solutions of (6), corresponding to two possible independent combinations of assignments of potential to the two strips. In view of the mirror symmetry, it is natural to choose the two solutions to be odd and even, respectively, with respect to reflection in the central xy plane of the cell. Under the substitution $z \rightarrow -z$, (6) is not invariant because of the presence of the first-order derivative which appears as a consequence of the form of z dependence assumed in (5). It is invariant, however, under the simultaneous substitutions $z \rightarrow -z$ and $f \rightarrow f^*$, where * denotes the complex conjugate. We may therefore choose two symmetry-adapted functions according to

$$\begin{aligned} f_o(y,-z) &= -f_o^*(y,z) \\ f_e(y,-z) &= +f_e^*(y,z) \end{aligned} \tag{11}$$

where o and e refer to the designations odd and even, respectively.

With the boundary conditions for the infinite array of parallel strips completely specified as described in the preceding, it is convenient to determine the distribution of charge and current on the conducting strips in two stages. The first stage is the determination of a Green's function appropriate to the dielectric-conductor configuration of the unit cell. As in former applications of this method [3], the Green's function may be taken to represent the potential created by a very narrow uniformly charged elementary substrip. (For computational purposes, sources of finite width are more convenient than the singular line sources ordinarily associated with the analytic concept of the Green's function.) The second stage in the determination of the normal modes on the array of parallel strips is the subdividing of each strip into a number of such narrow elements, and, with use of the Green's function which specifies the potential per unit charge at the location of each element, determining the charge distribution required to make the cross section of each conducting strip equipotential.

Let a substrip of width a be centered at z' and furnished with charge of uniform surface density σ. (It is anticipated that the width W of the strips themselves will be set equal to a multiple, say N, times the substrip width a.) The boundary condition on D_y is

$$D_y^+ - D_y^- = \begin{cases} \sigma, & \mid z - z' \mid \leq a/2 \\ 0, & \mid z - z' \mid > a/2. \end{cases} \tag{12}$$

With the assumption of uniform charge density $\sigma = \lambda/a$ on the substrip, we obtain with the aid of (9), (10), and (12),

$$C_m = \frac{\lambda}{\epsilon_o \mid \beta_m \mid p} \exp(-i\beta_m z') \frac{\sin \beta_m a/2}{\beta_m a/2} \frac{1}{\sinh \mid \beta_m \mid H_1 \coth \mid \beta_m \mid (H_2 - H_1) + K \coth \mid \beta_m \mid H_1}.$$

Denote the resulting potential due to a single substrip by $g(y,z \mid H_1,z')$; we obtain

$$g(y,z \mid H_1,z') = \frac{1}{\epsilon_0}\sum_m \frac{\exp[i\beta_m(z-z')]}{|\beta_m| p}\,\frac{\sin \beta_m a/2}{\beta_m a/2}\,\frac{\sinh |\beta_m| y}{\sinh |\beta_m| H_1}\,\frac{1}{\coth |\beta_m| (H_2-H_1) + K \coth |\beta_m| H_1},$$

$$0 \le y \le H_1$$

$$\frac{1}{\epsilon_0}\sum_m \frac{\exp[i\beta_m(z-z')]}{|\beta_m| p}\,\frac{\sin \beta_m a/2}{\beta_m a/2}\,\frac{\sinh |\beta_m| (H_2-y)}{\sinh |\beta_m| (H_2-H_1)}\,\frac{1}{\coth |\beta_m| (H_2-H_1) + K \coth |\beta_m| H_1},$$

$$H_1 \le y \le H_2. \quad (13)$$

IV. NORMAL MODES ON AN INFINITE ARRAY

The Green's function determined as in (13) may now be applied to the problem of determining the parameters of the normal modes of propagation on the infinite array of parallel strips illustrated in Fig. 1.

The charge distribution on the N substrips of a strip of width W is given by $\lambda_n, n = 1,\cdots,N$. This distribution is required to fulfill the following conditions: that each strip cross section be equipotential, that the phase increment between the two sides of the unit cell equal φ, and that the potential satisfy the symmetry specification of (11). In view of the uniformity of strip spacing, for a mode of phase φ per unit cell there must be a phase difference between strips of $\varphi/2$ for an even mode, and for an odd mode $\varphi/2$ together with reversal of sign, i.e., altogether, a phase difference of $\varphi/2 + \pi$ for an odd mode. For the unit cell centered at $z = 0$ with strips centered at $z = \pm p/4$ we may set the potential equal to $\exp(+i\varphi/4)$ for the right strip and $\pm \exp(-i\varphi/4)$ for the left; $-$ for the odd and $+$ for the even modes.

Now let us suppose the strips divided into N substrips, with the nth substrip of the strip on the right side of the unit cell bearing charge of linear density λ_n, then $n = 1, \cdots, N$. Let

$$z_n = \frac{S}{2} + \frac{W}{N}(n - \tfrac{1}{2}), \qquad n = 1,\cdots,N. \quad (14)$$

The contribution to the potential at the position of the n'th substrip due to the charge on the nth is $\lambda_n g(H_1,z_{n'} \mid H_1,z_n)$. To determine the λ_n, we set the potential of the strip equal to $\exp(+i\varphi/4)$:

$$\sum_{n=1}^{N} [\lambda_n g(H_1,z_{n'} \mid H_1,z_n) \pm \lambda_n^* g(H_1,z_n, \mid H_{1'}-z_n)] = \exp(i\varphi/4), \qquad n' = 1,\cdots,N \quad (15)$$

where $-$ and $+$ refer to the odd and even modes, respectively. Solution of this $N \times N$ system for the N values of λ_n yields, for each φ, the charge (and current) distribution over the strip cross section. This is illustrated in Fig. 3(a) and (b), which shows the width p of the unit cell divided into 80 elements. In this and all of the following illustrations the substrate dielectric constant contemplated is $K = 6.50$ (beryllium oxide) and the strip configuration is given by $W/H_1 = 0.720$, $S/H_1 = 0.912$ (see Fig. 2), with the upper ground plane position given by $H_2/H_1 = 2.600$. For this computation, each strip has been divided into ten substrips, and the linear charge

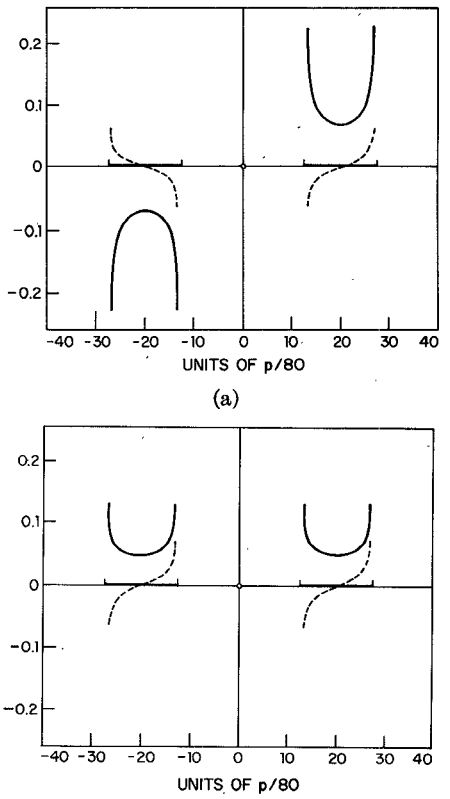

Fig. 3. Charge distribution λ_n, $N = 10$, on the two strips of the unit cell, for the normal modes at $\varphi = 20°$. (a) Odd mode. (b) Even mode. The linear charge density is expressed in picofarads per meter. The solid curves represent the real part; for the imaginary part, represented by the dashed curves, the scale is expanded $\times 10$.

density on each substrip is expressed in picofarads per meter. The value of φ is 20°. The solid curves represent the real part; for the imaginary part, represented by the dashed curves, the scale is expanded $\times 10$. The potential $U(H_1,z)$ at the substrate surface due to this charge distribution is shown in Fig. 4(a) and (b). The potential is expressed in volts. Here again, for the imaginary part, the scale is expanded $\times 10$.

The total charge Q

$$Q = \sum_{n=1}^{N} \lambda_n \quad (16)$$

is real. Since it corresponds to a potential of magnitude 1 V, it equals the capacitance per strip C_K, expressed in picofarads per meter. To complete the solution of this part of the problem in the quasi-TEM approximation, we

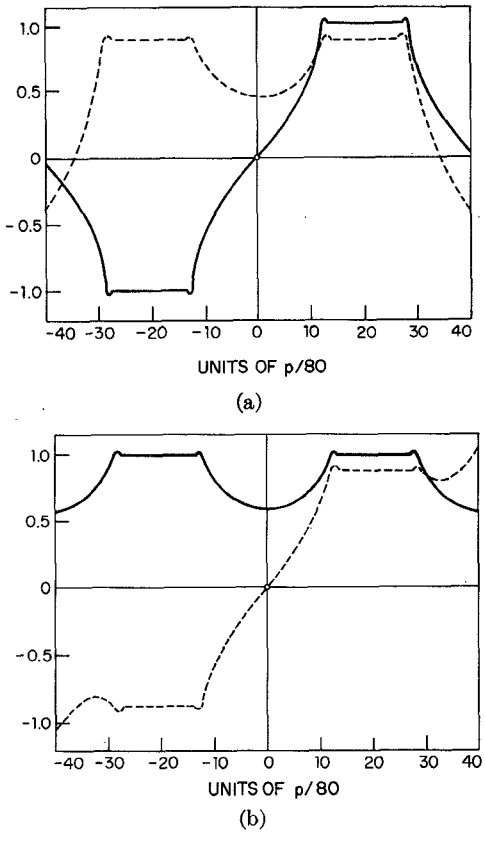

Fig. 4. Potential $U(H_1,z)$ in the unit cell for the normal modes at $\varphi = 20°$. (a) Odd mode. (b) Even mode. The potential is expressed in volts. The solid curves represent the real part; for the imaginary part, represented by the dashed curves, the scale is expanded $\times 10$.

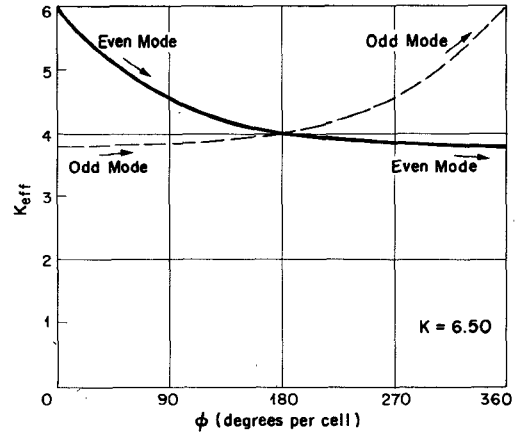

Fig. 5. Effective dielectric constant of the normal modes K_{eff} versus the phase per unit cell φ.

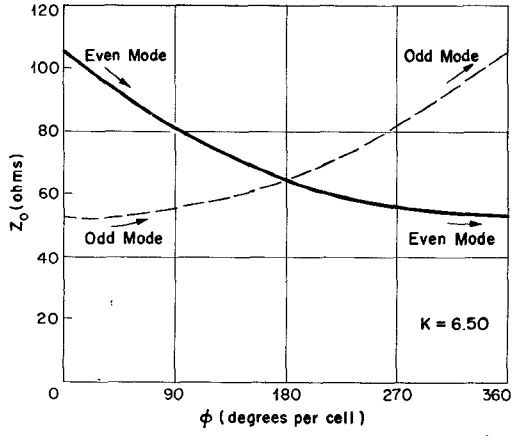

Fig. 6. Characteristic impedance of the normal modes Z_0 versus the phase per unit cell φ.

carry out the calculation of Q twice: once using the value K of the substrate dielectric constant contemplated, and again with K replaced by unity. The second calculation yields the vacuum capacitance C_1. The ratio C_K/C_1 is the effective dielectric constant K_{eff}. Fig. 5 shows K_{eff} as a function of φ for the illustrative example specified earlier with $K = 6.50$. We note that for the even mode at $\varphi = 0$ all the strips are at the same potential, namely, 1 V. There is very little fringing of the field between the strips into the vacuum above; consequently, the value of the effective dielectric constant, about $K_{eff} = 6.0$, is only slightly less than K itself. For the odd mode at $\varphi = 0$, on the other hand, the potential alternates between $+1$ and -1 V on successive strips; the field is concentrated between the edges of adjacent strips, where the dielectric is about equally composed of the substrate material and vacuum. Hence K_{eff} is roughly equal to the average value $(K + 1)/2 = 3.75$. With increasing φ the field distribution shifts from one of these two extremes to the other, with the fields of the two modes becoming identical at the center of the graph, at $\varphi = 180°$.

The velocity of propagation v is given by

$$\frac{v}{c} = (K_{eff})^{-1/2} \tag{17}$$

(where c is the characteristic velocity of empty space) and the normal-mode characteristic impedance Z_0 (Fig. 6) is

$$Z_0 = \frac{1}{vC_K} = \frac{1}{cC_1(K_{eff})^{1/2}}. \tag{18}$$

V. THE DISPERSION LAW FOR THE MEANDER LINE

We may visualize the meander line as having been formed by selecting a section of width A out of the infinite array of parallel strips and making connections at alternate ends, as illustrated in Figs. 1 and 2. In the present approximation we regard the connecting links as localized elements, disregarding their electrical length. More complicated assumptions regarding the length and scattering properties (or equivalent-circuit parameters) of the links can be treated within the scope of the present theory; such assumptions are capable of leading to improved realism, particularly with regard to the prediction of stopbands which are produced by the resultant effect of reflections from these regularly spaced obstacles. We shall see, however, that in the microstrip embodiment of the meander line, the existence and features of the stopbands are primarily associated with another effect, namely, the

difference in velocity between the even and odd modes, originating in their difference in field distribution in the inhomogeneous dielectric–vacuum medium, as described in the previous section.

We proceed to form waves satisfying the assumed boundary conditions at the connecting links by superposition of the normal modes. Considering the two strips in the unit cell, denoted by 1 and 2 for the left and right strip, respectively, we have the following voltages and currents:

$$\begin{aligned} v_1 &= [a_+ \exp(+ik_e x) + a_- \exp(-ik_e x) \\ &\quad - b_+ \exp(+ik_o x) + b_- \exp(-ik_o x)] \exp(-i\varphi/4) \\ v_2 &= [a_+ \exp(+ik_e x) + a_- \exp(-ik_e x) \\ &\quad + b_+ \exp(+ik_o x) - b_- \exp(-ik_o x)] \exp(+i\varphi/4) \end{aligned} \tag{19}$$

$$\begin{aligned} I_1 &= \{(1/Z_e)[a_+ \exp(+ik_e x) - a_- \exp(-ik_e x)] \\ &\quad + (1/Z_0)[-b_+ \exp(+ik_o x) - b_- \exp(-ik_o x)]\} \\ &\quad \cdot \exp(-i\varphi/4) \\ I_2 &= \{(1/Z_e)[a_+ \exp(+ik_e x) - a_- \exp(-ik_e x)] \\ &\quad + (1/Z_0)[b_+ \exp(+ik_o x) + b_- \exp(-ik_o x)]\} \\ &\quad \cdot \exp(+i\varphi/4) \end{aligned} \tag{20}$$

in which the coefficients $a_\pm$ and $b_\pm$ are the amplitudes of the even and odd modes, respectively, with propagation components in the $+x$ and $-x$ directions. Boundary conditions: if we make the simplest assumption, namely, to treat the connecting links as simple short circuits, we have

$$\begin{aligned} v_1(\tfrac{1}{2}A) &= v_2(\tfrac{1}{2}A) & I_1(\tfrac{1}{2}A) &= -I_2(\tfrac{1}{2}A) \\ v_2(-\tfrac{1}{2}A) &= v_3(-\tfrac{1}{2}A) & I_2(-\tfrac{1}{2}A) &= -I_3(-\tfrac{1}{2}A) \\ v_3(x) &= v_1(x) \exp(i\varphi) & I_3(x) &= I_1(x) \exp(i\varphi). \end{aligned} \tag{21}$$

If a more sophisticated assumption were to be introduced for the scattering effects of the discontinuities at the sides of the meander line, the appropriate impedance-matrix relation would replace the first two pairs of relations in (21). The third pair embodies the iterative phase assumption and would remain unchanged.

Equations (19) and (20), with the conditions (21), yield a system of homogeneous equations for the mode amplitudes $a_\pm$ and $b_\pm$. We put the system into the following form:

$$\begin{pmatrix} -i\epsilon_e T & -iT/\epsilon_e & -\epsilon_o & 1/\epsilon_o \\ iT/\epsilon_e & i\epsilon_e T & -1/\epsilon_o & \epsilon_o \\ i\eta\epsilon_e/T & -i\eta/\epsilon_e T & -\epsilon_o & -1/\epsilon_o \\ -i\eta/\epsilon_e T & i\eta\epsilon_e/T & -1/\epsilon_0 & -\epsilon_o \end{pmatrix} \begin{pmatrix} a_+ \\ a_- \\ b_+ \\ b_- \end{pmatrix} = 0 \tag{22}$$

where $T = \tan \varphi/4$, $\epsilon = \exp(ikA/2)$, and $\eta = Z_o/Z_e$. Here and in (20) the subscript o of (18) has been replaced by o and e for the odd and even mode species.

The characteristic equation for the system (22), which constitutes the dispersion law of the microstrip meander line, is

$$\tan^2 \frac{\varphi}{4} = \frac{Z_o}{Z_e} \begin{cases} \tan k_e A/2 \tan k_o A/2 \\ \cot k_e A/2 \cot k_o A/2 \end{cases} \tag{23}$$

with the upper and lower equations yielding alternately the successive forward- and backward-wave branches of the dispersion diagram, which is shown in Fig. 7. In the figure, the solid curves represent solutions of (23). The microstrip embodiment assumed for this illustration is the same as that for Figs. 3–6. As described before, the specifications are as follows:

$$\begin{aligned} K &= 6.50 \\ H_1 &= 0.0625 \text{ in} \\ A &= 0.492 \text{ in} \\ W/H_1 &= 0.720 \\ S/H_1 &= 0.912 \\ H_2/H_1 &= 2.60. \end{aligned}$$

In Fig. 7, the slanting dashed lines represent the effect of neglecting the coupling between the parallel strips of the meander line.

A meander-line slow-wave structure of the preceding specifications was tested at Lincoln Laboratory; the observed phase values, determined by a resonance method, are represented by the open points in Fig. 7, and the observed stopbands are represented by the horizontal dashed bars. To observe the phase per unit cell as a function of frequency, a section ten unit cells in length was prepared. The substrate is the ceramic beryllium oxide, and the circuit and ground plane are "chrome-gold"

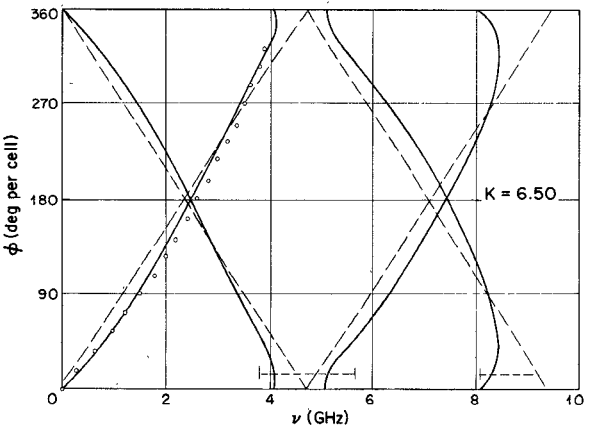

Fig. 7. Dispersion diagram for the microstrip meander line. As discussed in the text, the points and horizontal dashed bars are, respectively, the experimentally observed phase values and stopbands. The solid curves represent solutions of (23). The slanting dashed lines represent the limiting case of uncoupled meander lines.

prepared by photolithographic techniques. The upper ground plane is a separate brass plate. The section was placed in a resonator with large conducting walls at both ends, and was excited by a swept-frequency signal generator in the range from 0.1 to 8 GHz. A "comb" of resonances was observed. By probing the RF field, the order (number of wavelengths) was determined, and the frequency of each was observed with a cavity wavemeter. From the order of each resonance, the phase per unit cell was evaluated. In a separate measurement of insertion loss of the meander line, the frequency ranges of the stopbands were observed.

Stopbands are to be expected in a periodic structure of this type at those frequencies for which the phase difference between successive discontinuities is an integer multiple of 180°. For microstrip there is an additional influence leading to the appearance of stopbands, as is apparent from the dispersion equation (23). The effective dielectric constant values are in general different for the odd and even modes; therefore, so also are the propagation constants k_o and k_e. At frequencies for which the arguments $k_oA/2$ and $k_eA/2$ are in different quadrants (such as $k_oA/2 < 90°$ and $k_eA/2 > 90°$, as occurs in the vicinity of 4.7 GHz in Fig. 7) the right-hand side of (23) is negative, which requires that the phase parameter φ be imaginary; i.e., propagation is cut off. This phenomenon is obviously a distinctive characteristic of microstrip or of transmission media which share the property of inhomogeneity as represented in Fig. 5.

Solution of the system (22) also yields the mode composition of the meander-line field, namely,

$$a_+ = a_- \qquad b_+ = b_- \tag{24}$$

and

$$\frac{b}{a} = \mp \left(\frac{Z_o \sin k_eA}{Z_e \sin k_oA}\right)^{1/2} \tag{25}$$

in which, according to (24), the sign designations on a and b may be dropped. The double sign in (25) corresponds to the two dispersion branches of (23) (the minus sign goes with the fundamental forward-wave branch). We may deduce a meander-line image impedance (Fig. 8),

$$Z_{\text{in}} = \frac{v_1(0)}{I_1(0)} = \begin{cases} \left(Z_eZ_o \dfrac{\tan k_oA/2}{\tan k_eA/2}\right)^{1/2} \\ -\left(Z_eZ_o \dfrac{\cot k_oA/2}{\cot k_eA/2}\right)^{1/2} \end{cases}$$

where, of the two alternatives corresponding to the two branches of the dispersion diagram, the upper goes with the fundamental forward-wave branch.

VI. THE INTERACTION IMPEDANCE

As defined, for example, by Mourier [6], the interaction impedance Z_{int} is

$$(Z_{\text{int}})_m = (1/2P\beta^2)\ \text{Im}\ (E_{ym}E_{zm}^*)$$

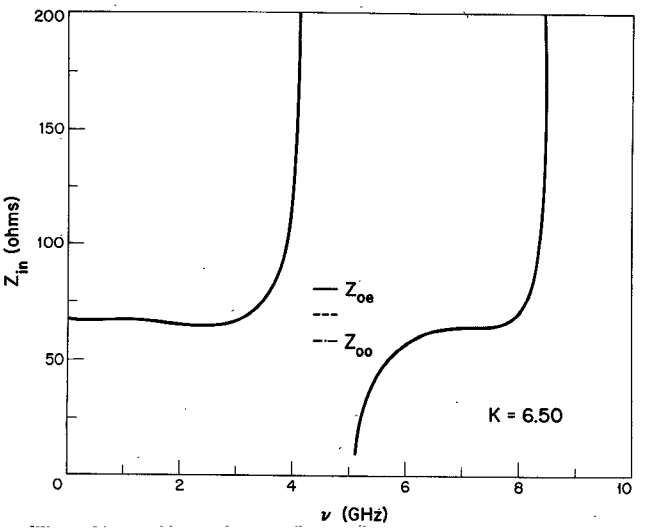

Fig. 8. Image impedance Z_{in}. The three bars in the center of the figure indicate for comparison the characteristic impedances of a coupled pair of lines [3] of the same configuration (upper and lower bars) and of a single line (center bar).

where E_{ym} and E_{zm} are the mth spatial Fourier component (mth space harmonic) of the microwave electric field at a specified level in the interaction region above the meander-line surface; P is the microwave power, and $\beta = \varphi/p$ is the propagation constant for propagation in the meander-line z direction.

A parameter of the character of Z_{int}, such as that defined in [6] and in a slightly different manner in [2], has long been employed in the theory of beam-type vacuum tubes to characterize the coupling between the RF electromagnetic field and the electron beam in the interaction region above the slow-wave structure, in such a way as to provide a measure of the net rate of RF power amplification, at least in the limit of small RF signal amplitude.

To determine the power flow, the group velocity must be evaluated with the aid of the dispersion relation, and the electromagnetic energy density must be determined through use of the capacitance; the principles are essentially the same as those presented in [2]. The result for the present meander-line formulation is

$$P = \frac{2A}{p} v_g \left[\frac{|a|^2}{v_eZ_e}\left(1 + \frac{\sin k_eA}{k_eA}\right) + \frac{|b|^2}{v_oZ_o}\left(1 - \frac{\sin k_oA}{k_oA}\right)\right].$$

The components of the electric field at the specified location in the interaction region are available directly by differentiation of the potential $\Phi(x,y,z)$ determined earlier in Sections II–V.

An example of the interaction impedance is presented in Fig. 9. Z_{int} in the figure is for the meander-line configuration illustrated in the previous figures, for the level $y = H_1$, i.e., at the substrate surface, and for $m = 0$; i.e., for the zero-order space harmonic. (The irregularity of the curve is due in part to the somewhat rough differentiation of the dispersion curve which was employed in determining the group velocity v_g.) This rather simple example is presented to illustrate the potential of the

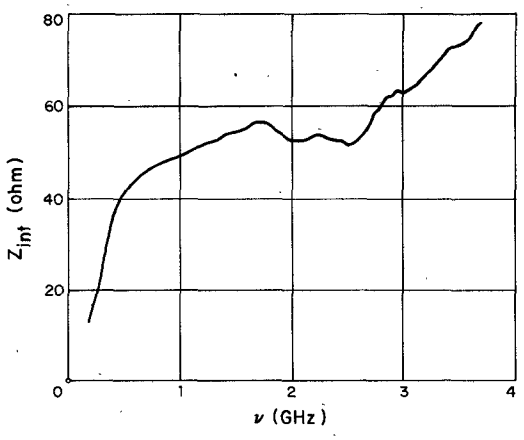

Fig. 9. Interaction impedance Z_{int} for the zero-order space harmonic $m = 0$ at the center of the substrate surface $(x,y) = (0,H_1)$.

present formulation in applications such as CFA development where accurate determination of the RF fields must be made in a relatively complicated inhomogeneous transmission line cross section.

VII. CONCLUSION

Computations carrying out the analysis presented earlier have been performed on the CP/CMS Time-Sharing System at MIT Lincoln Laboratory. In a first program, the Fourier-series formulation of the Green's function (13) is evaluated at the substrate surface $y = H_1$, and the system (15) is solved for the charge distribution. The output of this program is a table giving the even- and odd-mode velocities and characteristic impedances as functions of the iterative phase parameter φ. A second program uses these data as input to find, for each table entry, the corresponding frequency satisfying the characteristic equation (23). With this solution, constituting the dispersion law of the meander line, the fields, and all other parameters of the structure, are completely determined.

It is evident that this framework is not limited to the present example of the meander line, but is suitable for the analysis of a wide range of complex periodic transmission line structures in the quasi-TEM regime. Beyond the immediate objective, namely, to obtain realistic data for comparison and design guidance on a class of slow-wave structures for crossed-field amplifier development, the formulation illustrates how a technique for systematic accounting of the complex fields in a periodic medium can be carried out by a combination of logical, analytical, and computational methods.

ACKNOWLEDGMENT

The author wishes to thank D. H. Temme for his interest and encouragement and W. E. Courtney for the benefit of valuable discussions on aspects of this work.

REFERENCES

[1] J. Arnaud, "Circuits for traveling wave crossed-field tubes," in *Crossed-Field Microwave Devices*, Okress *et al.*, Ed. New York: Academic, 1961, ch. 2.3.
[2] P. N. Butcher, "The coupling impedance of tape structures," *Proc. Inst. Elec. Eng.*, vol. 104B, p. 177, 1957.
[3] T. G. Bryant and J. A. Weiss, "Parameters of microstrip transmission lines and of coupled pairs of microstrip lines," *IEEE Trans. Microwave Theory Tech. (1968 Symposium Issue)*, vol. MTT-16, pp. 1021–1027, Dec. 1968.
[4] L. Brillouin, *Wave Propagation in Periodic Structures.* New York: McGraw-Hill, 1946, p. 140.
[5] *IEEE Trans. Microwave Theory Tech. (Special Issue on Computer-Oriented Microwave Practices)*, vol. MTT-17, pp. 414–660, Aug. 1969; also, *IEEE Trans. Microwave Theory Tech. (Special Issue on Computer-Oriented Microwave Practices)*, vol. MTT-22, pp. 153–351, Mar. 1974.
[6] G. Mourier, "Small signal theory," in *Crossed-Field Microwave Devices*, Okress *et al.*, Ed. New York: Academic, 1961, p. 406.